

Accurate fitting of a Multi-Pool Proton Exchange System with a Priori Fitted Two-Pool MTC Information

Hye-Young Heo¹, Yi Zhang¹, Dong-Hoon Lee¹, Xiaohua Hong¹, and Jinyuan Zhou¹

¹Russell H Morgan Department of Radiology and Radiological Science, Johns Hopkins University, Baltimore, Maryland, United States

Introduction

CEST imaging is an important molecular MRI technique that can generate contrast based on the saturation transfer between bulk water protons and low-concentration solute labile protons¹. Because RF radiation to saturate the solute labile protons induces large direct water saturation and conventional MT from semi-solid macromolecules, the quantitative CEST measurement and theoretical simulation are complicated²⁻⁵. In this study, we investigated the mixed MT, APT, and NOE effects in a multi-pool proton exchange model with the *a priori* fitted two-pool MTC information.

Methods

Six human glioblastoma-bearing adult Fisher 344 rats were scanned on a horizontal bore Bruker 4.7 T. CEST image data were obtained using a fat-suppressed spin-echo pulse sequence with a single-shot EPI readout (TR = 10 s; TE = 30 ms; matrix size = 64 x 64 mm²; FOV = 32 x 32 mm²; slice thickness = 1.5 mm; and RF saturation time = 4 s). Two sets of z-spectra with 26 frequency offsets were acquired to quantify conventional MT, NOE, and APT effects, using three RF saturation powers (0.5, 1.3, and 2.1 μ T): (1) $Z_{21 \sim -21 \text{ ppm}}$: 21 to -21 ppm at intervals of 1.75 ppm for MT modeling with the super-Lorentzian lineshape; (2) $Z_{6 \sim -6 \text{ ppm}}$: 6 to -6 ppm at intervals of 0.5 ppm for the

quantification of NOE and APT effects. The wide-offset data were fitted to two-pool MT model with the super-Lorentzian lineshape². Data points of small frequency offsets between 7 and -7 ppm in B_0 -corrected $Z_{21 \sim -21 \text{ ppm}}$ were excluded ($Z_{21 \sim -21 \text{ ppm}}$) to avoid

APT and most NOE contributions prior to conventional MT modeling. Next, a four-pool exchange model was analytically solved with the fitted two-pool MT information, and the parameter fitting was performed using the minimum norm estimate. The post-hoc test was performed for $p < 0.05$: <: significantly smaller; >: significantly larger; not indicated: no significant difference.

Results and Discussion

The two-pool MT model accurately fitted the behavior of the semi-solid MT system for wide frequency offsets as shown in Fig. 1. The MT parameters (except T_{2m}) were significantly different between the normal tissue and the tissue in the tumor center or rim as shown in Table 1. Four-pool APT and NOE exchange model fitted the $Z_{6 \sim -6 \text{ ppm}}$ behavior very well as shown in Fig. 2. As expected (Table 2), the APT-related pool sizes of the tumor center and the tumor rim were significantly larger than that of the normal tissue, while the NOE-related pool sizes of the tumor center and the tumor rim were significantly smaller than that of the normal tissue.

Further, by subtracting experimental data ($Z_{6 \sim -6 \text{ ppm}}$) or simulated four-pool data from Z_{EMR} , APT[#] and NOE[#] signals could be obtained (Fig. 3). The APT[#] signals in all ROIs were lowest at the RF saturation power of 0.5 μ T and seemingly peaked at 1.3 μ T, while the NOE[#] signals were lowest at 2.1 μ T. The APT[#] signals of the tumor center and the tumor rim were both significantly higher than those of the normal tissue across all power levels ($p < 0.05$). The NOE[#] signals were generally lower in the tumor center and rim than in the normal tissue, which reached statistical significance ($p < 0.05$) in the tumor center at 1.3 μ T.

Conclusions

Four-pool fitting using extrapolated semi-solid MTC parameters as prior known information could reduce the over-fitting errors. The quantitative results would provide some insight into the mechanisms of APT and NOE effects in tissue.

References

1. Ward et al. JMR 143:79 (2000).
2. Li et al. MRM 60:1197 (2008).
3. Zaiss M, et al. JMR 211:149 (2011).
4. Liu et al. MRM 70:1070 (2013).
5. Desmond KL, et al. MRM 71:1841 (2014).
6. Henkelman et al. MRM 29:759 (1993).

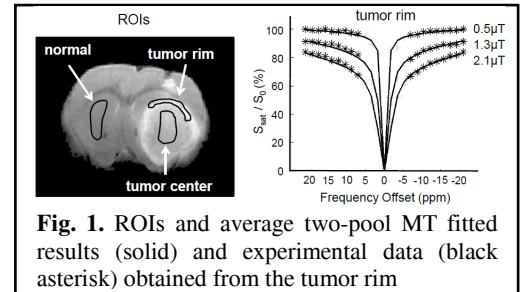


Fig. 1. ROIs and average two-pool MT fitted results (solid) and experimental data (black asterisk) obtained from the tumor rim

$n=6$	R (s^{-1})	T_{2m} (μ s)	$RM_0^m T_{1w}$	T_{1w}/T_{2w}	T_{2w} (ms)	T_{1w} (s)	T_{1w}^{obs} (s)	M_0^m (%)
Normal	17.7 ± 0.8	18.7 ± 1.6	2.17 ± 0.15	44.6 ± 0.5	31.5 ± 0.4	1.40 ± 0.02	1.36 ± 0.02	8.7 ± 0.7
Tumor center	20.3 ± 1.3	19.8 ± 0.4	1.39 ± 0.14	39.4 ± 0.9	50.0 ± 0.9	1.97 ± 0.05	1.91 ± 0.05	3.6 ± 0.3
Tumor rim	21.5 ± 1.1	18.5 ± 1.2	1.34 ± 0.04	29.9 ± 0.5	64.7 ± 0.8	1.93 ± 0.04	1.88 ± 0.05	3.1 ± 0.2
Post-hoc	$N < TC, TR$		$N > TC, TR$	$N > TC > TR$	$N < TC < TR$	$N < TC, TR$	$N < TC, TR$	$N > TC > TR$

w: free bulk water, *m*: semi-solid macromolecule, *R*: exchange rate between two pools, *M*₀: proton pool size

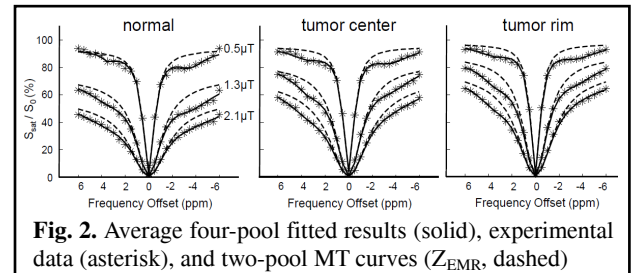


Fig. 2. Average four-pool fitted results (solid), experimental data (asterisk), and two-pool MT curves (Z_{EMR} , dashed)

$n=6$	Amide proton pool (S_1)			NOE-related proton pool (S_2)		
	M_0^{S1} (%)	k_{S1w} (Hz)	T_{2s1} (ms)	M_0^{S2} (%)	k_{S2w} (Hz)	T_{2s2} (ms)
Normal	0.31 ± 0.03	23.9 ± 6.8	11.5 ± 1.1	0.66 ± 0.22	16.3 ± 8.3	0.40 ± 0.1
Tumor center	0.39 ± 0.03	21.5 ± 2.5	10.1 ± 3.4	0.39 ± 0.07	17.6 ± 4.1	0.38 ± 0.2
Tumor rim	0.40 ± 0.05	28.3 ± 9.6	11.2 ± 2.5	0.36 ± 0.13	15.4 ± 5.8	0.39 ± 0.4
Post-hoc	$N < TC, TR$			$N > TC, TR$		

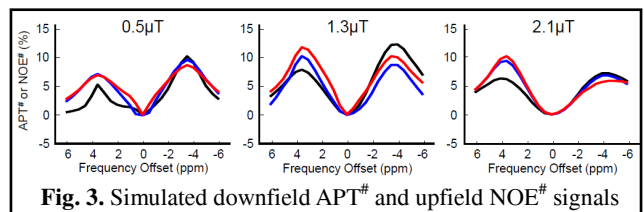


Fig. 3. Simulated downfield APT[#] and upfield NOE[#] signals